

AFRL-IF-RS-TR-2000-36
Final Technical Report
April 2000



PHOTO-ELECTRONIC OPTICAL MEMORY WRITE/READ SYSTEM

Nanogen, Inc.

Michael Heller

APPROVED FOR PUBLIC RELEASE; DISTRIBUTION UNLIMITED.

20000420 068

**AIR FORCE RESEARCH LABORATORY
INFORMATION DIRECTORATE
ROME RESEARCH SITE
ROME, NEW YORK**

DTIC QUALITY INSPECTED 3

This report has been reviewed by the Air Force Research Laboratory, Information Directorate, Public Affairs Office (IFOIPA) and is releasable to the National Technical Information Service (NTIS). At NTIS it will be releasable to the general public, including foreign nations.

AFRL-IF-RS-TR-2000-36 has been reviewed and is approved for publication.

APPROVED:



EDWARD DANISZEWSKI
Project Engineer

FOR THE DIRECTOR:



JOHN V. MCNAMARA, Technical Advisor
Information & Intelligence Exploitation Division
Information Directorate

If your address has changed or if you wish to be removed from the Air Force Research Laboratory Rome Research Site mailing list, or if the addressee is no longer employed by your organization, please notify AFRL/IFED 32 Brooks Road, Rome, NY 13441-4114.. This will assist us in maintaining a current mailing list.

Do not return copies of this report unless contractual obligations or notices on a specific document require that it be returned.

REPORT DOCUMENTATION PAGE			Form Approved OMB No. 0704-0188	
<small>Public reporting burden for this collection of information is estimated to average 1 hour per response, including the time for reviewing instructions, searching existing data sources, gathering and maintaining the data needed, and completing and reviewing the collection of information. Send comments regarding this burden estimate or any other aspect of this collection of information, including suggestions for reducing this burden, to Washington Headquarters Services, Directorate for Information Operations and Reports, 1215 Jefferson Davis Highway, Suite 1204, Arlington, VA 22202-4302, and to the Office of Management and Budget, Paperwork Reduction Project (0704-0188), Washington, DC 20503.</small>				
1. AGENCY USE ONLY (Leave blank)		2. REPORT DATE APRIL 2000		3. REPORT TYPE AND DATES COVERED Final Jun 97 - Jun 99
4. TITLE AND SUBTITLE PHOTO-ELECTRONIC OPTICAL MEMORY WRITE/READ SYSTEM			5. FUNDING NUMBERS C - F30602-97-C-0229 PE - 62702F PR - 4594 TA - 97 WU - 24	
6. AUTHOR(S) Michael Heller				
7. PERFORMING ORGANIZATION NAME(S) AND ADDRESS(ES) Nanogen, Inc. 10398 Pacific Center Court San Diego CA 92121-4340			8. PERFORMING ORGANIZATION REPORT NUMBER N/A	
9. SPONSORING/MONITORING AGENCY NAME(S) AND ADDRESS(ES) Air Force Research Laboratory/IFED 32 Brooks Road Rome NY 13441-4114			10. SPONSORING/MONITORING AGENCY REPORT NUMBER AFRL-IF-RS-TR-2000-36	
11. SUPPLEMENTARY NOTES Air Force Research Laboratory Project Engineer: Edward Daniszewski/IFED/(315) 330-4466				
12a. DISTRIBUTION AVAILABILITY STATEMENT APPROVED FOR PUBLIC RELEASE; DISTRIBUTION UNLIMITED.			12b. DISTRIBUTION CODE	
13. ABSTRACT (Maximum 200 words) Chromophoric DNA polymers are being developed for high density optical data storage applications. This project involves the design and synthesis of chromophoric DNA polymers which absorb light energy at a single wavelength and re-emit at predetermined multiple wavelengths. By emitting spectra rather than binary on/off bits, the data word size can be increased significantly and parallel access is enabled. The diffraction limit normally experienced with classical optical interrogation of a binary data site can now be overcome, because the number of data bits per unit area is increased in relation to the number of wavelengths produced at that site. In relation to this DNA optical memory project, a potentially more powerful write process is now being proposed for incorporating higher bit/byte densities in these DNA optical materials. This process, called a "photo-electronic write", involves using spatial light addressing to a photoactive substrate material which creates microscopic electric fields. These electric fields affect the rapid transport and attachment of charged chromophoric (color) DNA's to the selected write locations. The "photo-electronic write process" has advantages over this earlier UV write process for the optical storage systems, with potential capacities approaching petabytes on a 5 1/4" disc.				
14. SUBJECT TERMS DNA, Oligonucleotides, Chromophores			15. NUMBER OF PAGES 36	
			16. PRICE CODE	
17. SECURITY CLASSIFICATION OF REPORT UNCLASSIFIED	18. SECURITY CLASSIFICATION OF THIS PAGE UNCLASSIFIED	19. SECURITY CLASSIFICATION OF ABSTRACT UNCLASSIFIED	20. LIMITATION OF ABSTRACT UL	

Table of Contents

I.	Summary	3
II.	Objectives & Approach	4
III.	Contract Requirements	5
IV.	Contract Execution	6
V.	Conclusions	25
	Appendix A	26
	Appendix B	27

List of Figures

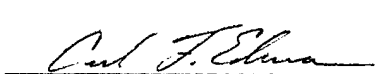
Figure 1	Schematic view of the optical write platform	7
Figure 2	Schematic top-view of the electrochemical setup	7
Figure 3	Cyclic voltammogram of n-type Si etched with buffered HF	8
Figure 4	Cyclic voltammograms of a) n-type Si covered with <20nm PT	9
Figure 5	Calculated %transmission of Pt and Pd thin films for light	9
Figure 6	Platinum and palladium patterns on n-type silicon substrates	10
Figure 7	Cyclic voltammograms of a) n-type silicon with 2nm Pd	10
Figure 8	Cyclic voltammograms of a) n-type Si covered with thin layers	11
Figure 9	AFM surface plot of a $\text{Mn}_2\text{-O}_3$ thin film	12
Figure 10	AFM profile of the edge region of a $\text{Mn}_2\text{-O}_3$ thin film	12
Figure 11	a) Fluorescent DNA oligonucleotide accumulation	13
Figure 12	Polypyrrole lilnes produced by the photo-electrochemical write	14
Figure 13	Bead movement induced by photo-electrochemical currents	15
Figure 14	Accumulation of 1um diameter polystyrene beads	15
Figure 15	Cyclic voltammogram of Mn_2O_3 stabilized silicon substrate	16
Figure 16	Schematic view of the structure of the photowrite platform	17
Figure 17	Basic configurations for the introduction of fluorescent dyes	18
Figure 18	Absorption and emission spectra of fluorescent dyes used	19
Figure 19	Effect of 650 nm laser irradiation during electronic binding	19
Figure 20	Fluorescent patterns produce by the photowrite process	20
Figure 21	Fluorescence intensity contour plots of photowrite patterns	21
Figure 22	Not Available	
Figure 23	Not Available	
Figure 24	Combination of dyes and oligonucleotides demonstrating	22
Figure 25	Example of a two color photowrite pattern	22

I. Summary

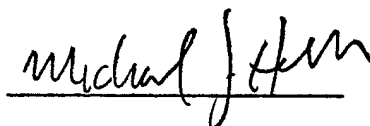
The project objective was the creation of a photo-controlled, microarray-independent means of patterning fluorescently labeled deoxyribonucleic acid (DNA) oligonucleotides using electric fields. The development of photo-directed movement of molecular (and micron) scale materials in an aqueous solution overlaying a photoreactive surface was central to this objective. This photo process can be described as follows: by irradiating a small portion of a photoreactive surface in the presence of an applied potential, a current through the solution is created, originating at the surface of the photodiode at the point of illumination and terminating at the counter electrode, also in solution. This photo generated current creates an electrophoretic force allowing the controlled transport of charged species through the solution, thus giving rise to the term "photo-electrophoresis". In order to accomplish this, an optical platform incorporating a single-mode optical fiber mounted on an electronic micropositioning system was assembled. The fiber optic produced an illuminated spot size of about 10-30 μm . Using this platform, a number of possible surfaces were tested for photoreactivity and stability in an aqueous environment. Of these, the surface created by the deposition of a thin film of Mn_2O_3 onto a pretreated n-type single-crystal silicon substrate was selected for further work. Attachment sites for DNA oligonucleotides on this surface were obtained by casting a thin streptavidin containing hydrogel permeation layer on top of the Mn_2O_3 film. DNA oligonucleotides labeled with fluorescent probes were photo-electrophoretically moved to specific locations on the photoactive surface and attached to the permeation layer by the interaction between biotin (attached to the DNA strand) and streptavidin (located in the permeation layer). Additional oligonucleotides were hybridized to these previously localized oligonucleotides. With this process, two color fluorescent spots and lines were successfully written onto the substrate and read out using either a high-resolution optical scanner or a CCD camera with laser illumination. This patterning of optically active materials might ultimately serve as a means to encode forms of information based upon wavelengths and distribution of the fluorescent groups. In conclusion, this project has demonstrated controlled photo-electrophoresis of micron and molecular scale materials and the targeted assembly of fluorescently labeled DNA oligonucleotides using freely positioned laser illumination.



Christian Gurtner, Ph.D.
(principal scientist)



Carl Edman, Ph.D.
(program manager)



Michael J. Heller, Ph.D.
(chief technical officer)

II. Objectives & Approach

One of the limiting factors in developing high density optical memory systems is the optically active read/write storage material. Conventional materials, such as those used in CD-ROM technology, have a "0" or "1" response to incident laser light, i.e., an illuminated spot that is either reflecting or non-reflecting. Other optical properties, e.g. absorption and emission wavelengths, intensity and polarization, are tunable and measurable. These are potentially more useful for information storage than simple reflectance. That is, by employing one or all of these properties, a single storage location should be able to contain multiple bits of information instead of just one. Overall, this should result in dramatically increased information storage density.

As one step towards this long term goal, this project was created to explore a novel means to electronically arrange DNA-based optical components. In particular, the core idea is to use photo-controlled electrophoretic transport through a solution overlaying a photoactive surface to specifically target charged materials, e.g. DNA, to the photosurface at the site of illumination. This differs from Nanogen's base technology on which transport and specific localization of micron to molecular scale materials and devices is done using precisely constructed and individually controllable microelectrode arrays. These microelectrodes are conventional in the sense that they reproduce conventional macroscale electrophoresis, albeit on a much smaller scale. However, this microelectrode approach is limited by the geometry and scale of the array. A much more flexible system allowing greater packing density would be forthcoming if the electrophoretic process did not depend on microelectrodes and their associated electrical interconnects. In addition, the chip itself would be more amenable and cheaper to manufacture if formed from simple layers without the necessity for multiple patterned layers composed of diverse materials.

To develop this, three necessary components have to be integrated into one package -

- a photo-reactive surface stable to aqueous electrophoresis must be developed.
- suitable oligonucleotide attachment chemistry to this surface has to be found.
- an apparatus for writing to this surface and reading from this surface needs to be assembled.

These three components are more precisely defined as discreet elements of the Statement of Work (SOW) objectives in the following section outlining the contract requirements.

Extensive use of Nanogen's base technology was employed, when appropriate, to expedite progress towards contract goals. This includes knowledge of DNA oligonucleotide synthesis and derivatization with fluorescent dyes, permeation layer development, fluorescent energy transfer and experience in the micro-electrophoretic transfer and attachment of DNA molecules in low-conductivity solutions.

III. Contract Requirements

(underlined numbers refer to original SOW objectives)

- a) Design and Synthesis of Oligonucleotides: 4.1.1 Design, synthesize, and purify DNA attachment sequences and DNA chromophore labeled sequences.
- b) Development of a Photoactive Substrate: 4.1.1.1 Evaluate and test photoactive substrate materials for active transport of DNA molecules in electrolyte solutions.
- c) Attachment of DNA Oligonucleotides: 4.1.1.2 Attach DNA sequences to selected photoactive substrate materials.
- d) Demonstrate the Photowrite Process: 4.1.2 Demonstrate the photo-electronic write process on DNA sequences attached to photoactive substrate materials. 4.1.3 Demonstrate spectral read-out process of DNA sequences attached to photoactive substrate materials. 4.1.4 Optimize the size of the write locations (4.1.2) and demonstrate the photo-electric write/read process in pixel format.
- e) Demonstration/Reports/Evaluation: 4.1.5 Deliver a photo-electric write/read breadboard model demonstration system. 4.1.6 Continually determine the status of the effort and report progress towards accomplishment of contract requirements. 4.1.7 Conduct oral presentations at such times and places designated in the contract schedule. Provide status of technical progress made to date in performance of the contract during presentations. Contractor presentations will be attended by approximately two (2) Government personnel. 4.1.8 Conduct an experimental demonstration exhibiting paragraphs 4.1.2 and 4.1.3; and an experimental demonstration exhibiting paragraph 4.1.4 at the end of the contract period. Document each experiment on video tape.
- f) Documentation: 4.1.9 Document all technical work accomplished and information gained during performance of this acquisition. Include all pertinent observations, nature of problems, positive and negative results, and design criteria established where applicable. Document procedures followed, processes developed, "Lessons Learned," etc. Document the details of all technical work to permit full understanding of the techniques and procedures used in evolving technology or process developed. Cross-reference each design, engineering, or process specification delivered to permit a full understanding of the total acquisition.

IV. Contract Execution

a) Design and Synthesis of DNA Oligonucleotides: 4.1.1 Design, synthesize, and purify DNA attachment sequences and DNA chromophore labeled sequences.

A number of DNA oligonucleotides were designed and synthesized exclusively for this project (Appendix A). In addition, we had access to other nucleotides at Nanogen which had been previously synthesized for other projects and purposes. As needed, oligonucleotides were derivatized, using standard techniques, with the following fluorescent chromophores purchased from Molecular Probes, Inc.: BODIPY TR-X (absorption 588 nm, emission 616 nm); BODIPY 493/503 (absorption 490 nm, emission 503 nm) and BODIPY 630/650-X (absorption 630, emission 650 nm).

b) Development of a Photoactive Substrate: 4.1.1.1 Evaluate and test photoactive substrate materials for active transport of DNA molecules in electrolyte solutions.

In order to evaluate various photoactive materials, an optical write setup, schematically shown in Figure 1, was designed and assembled. The working end consists of a single-mode fiber (8 μm diameter) mounted on a programmable, motorized Eppendorf XYZ micromanipulator stage above a simple electrochemical cell (Figure 2). The light source was a laser (2.5 mW 594 nm HeNe or 10 mW 630 nm HeNe) coupled into the single mode fiber using a free launch configuration (measured coupling efficiency with minimal laser destabilization >16%). This free launch configuration allowed for attenuation of the light intensity using a neutral density filter wheel as well as allowing "chopping" of the laser beam. Typically the laser light was attenuated to produce illumination intensities on the chip of 10-250 μW . On the chip, the single mode fiber produces a minimal illumination spot-size of approximately 15 μm (fiber immersed into solution). This electrochemical cell plus fiber optic was placed underneath a microscope equipped with a sensitive color CCD camera for real-time monitoring. An additional 150 W halogen white light source was used for substrate stability measurements (not shown in Figure 1).

The reading step was performed using a different platform than the one described above for writing. This reader was either on a high-resolution fluorescence scanner (Molecular Dynamics) or custom built in-house research instruments used at Nanogen for basic developmental projects. These instruments contain the necessary laser illumination, optical objectives, wavelength filters and computer interfaced, high sensitivity CCD cameras.

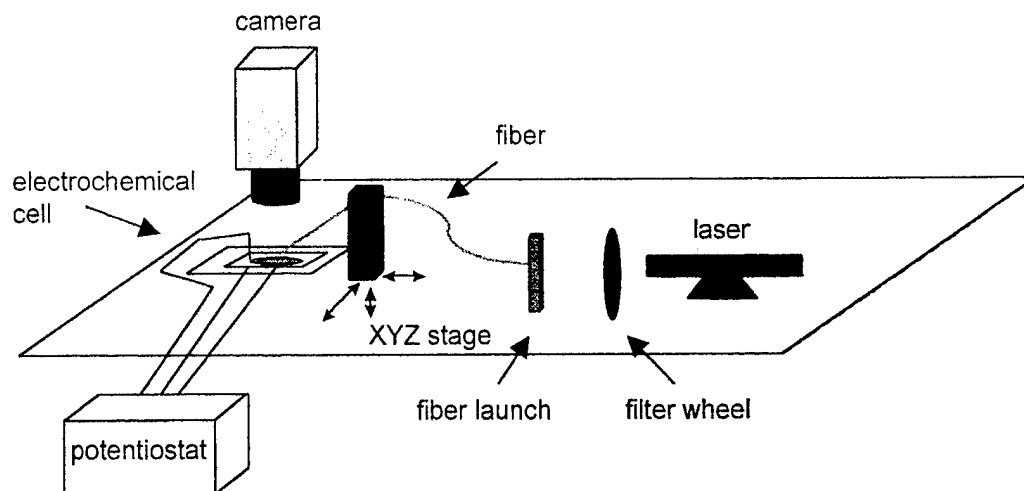


Figure 1. Schematic view of the optical write platform.

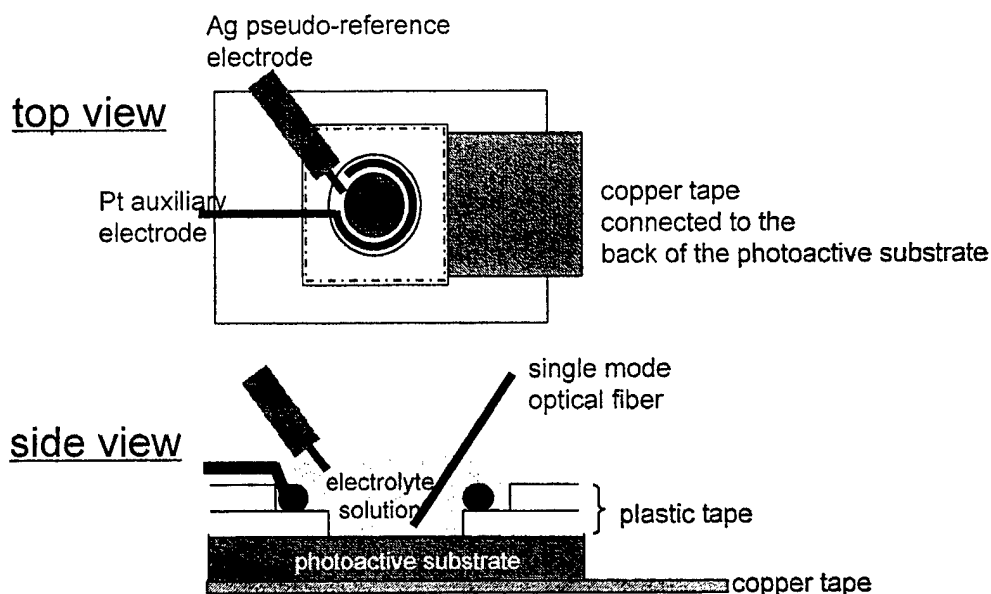


Figure 2. Schematic top-view of the electrochemical setup.

Having assembled a suitable test platform for examining photoactive materials, the choice of which of these materials to examine became the next priority. In general, inorganic and organic semiconductors are the materials of choice for the generation of photocurrents or photoelectrochemical currents. While there is a rich variety of semiconductors that are suitable for solid state devices (solar cells, photodiodes etc), only a limited selection of these are also adequate for photoelectrochemical current formation. Even worse, not a single semiconductor or compound semiconductor material is known that can withstand the

corrosive environment present during photooxidation of water. Unfortunately, photooxidation of water is needed for DNA electrophoresis in aqueous electrolytes and is the dominant process at the positive electrode (anode). Compounding these difficulties are other criteria required in a suitable photoactive substrate. In addition to stability, these include: low dark current; low lateral conductivity; high junction potential; and high photoconversion efficiency. The level of dark current has a direct influence on the signal to background ratio or the contrast of the photowrite process. Lateral conductivity or minority carrier diffusion can limit the obtainable resolution. Improvements in this respect could be expected from patterned (pixilated) surfaces. A high junction potential (typically 0.5 V for Si) is necessary to reach the electrochemical oxidation potential of water without having to apply a large bias. The photoconversion efficiency determines how much illumination power is needed to generate a desired photocurrent.

Unprotected semiconductor surfaces. Preliminary experiments with n-type single crystal silicon photoanodes in 50 mM histidine electrolyte solutions (an electrolyte used for electrophoretic DNA transport on microarrays) showed that the silicon surface becomes insulating and therefore photo-inactive within a few seconds. This effect was evaluated using cyclic voltammetry. In brief, cyclic voltammetry consists of applying a voltage of varying strength while simultaneously measuring the resultant current. An example is shown in Figure 3. In this experiment, the first voltage "sweep" exhibited a current in excess of 20 μA at the peak applied voltage. Subsequent voltage sweeps produced progressively lower currents. The lower currents indicate that the resistivity of the photo surface is constantly increasing, or in other words, an insulating layer is forming on the surface over time. Therefore, such a surface would be of limited use for prolonged photo write experiments. Similar negative results were obtained with np-junction photodiodes and indium-tin-oxide (ITO) electrodes.

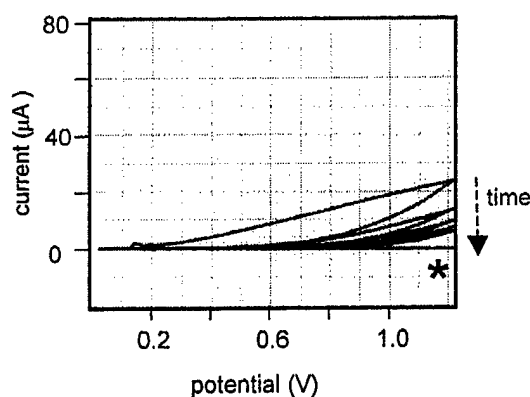


Figure 3. Cyclic voltammogram of n-type Si etched with buffered HF (photoresponse but poor stability)

To get around this rapid loss in surface performance shown by unprotected semiconductor surfaces, we examined the feasibility of protecting the surface with electrochemically inert yet electrically conductive coatings. These were based on the few published reports of stabilization of inorganic semiconductor photoanodes against corrosion in water by deposition of various protective surface layers. We reproduced some of these methods, e.g. platinum, palladium and Mn_2O_3 layers, for the protection of n-type single crystal silicon anodes.

Vapor deposition of patterned and unpatterned platinum thin films. The stabilizing effects of platinum thin films (< 20 nm) is controversial and, indeed, we did not see any significant stabilization of the silicon surface against oxidation (Figure 4a). Thicker platinum films (> 20 nm) were more stable but showed reduced photoresponse (absorption) and high background currents. (Figure 4b) The simplest explanation for reduced photoresponse is shown in Figure 5. This indicates that beyond 20 nm thickness, transmittance of light through the metal to the silicon is greatly reduced. [Calculated values for transmission of light with $\lambda = 630$ nm for various thicknesses of Pt or Pd ($k_{\text{Pt}} = 4.07$ and $k_{\text{Pd}} = 3.54$)] Not considered in this figure are those losses caused by reflection ($R_{\text{Pt}}=0.66$, $R_{\text{Pd}}=0.72$, $R_{\text{Si}} \approx 0.35$). Patterned films, shown in Figure 6, were as unstable as the unpatterned.

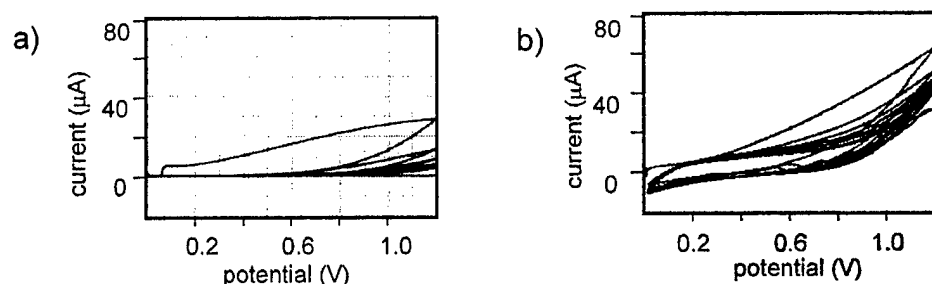


Figure 4. Cyclic voltammograms of a) n-type Si covered with < 20 nm Pt (photoresponse but poor stability) and b) n-type Si covered with >20 nm Pt (no photoresponse, but relatively stable).

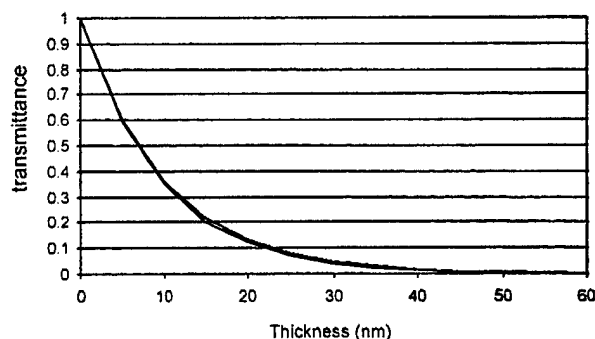


Figure 5. Calculated %transmission of Pt and Pd thin films for light with $\lambda=630$ nm.

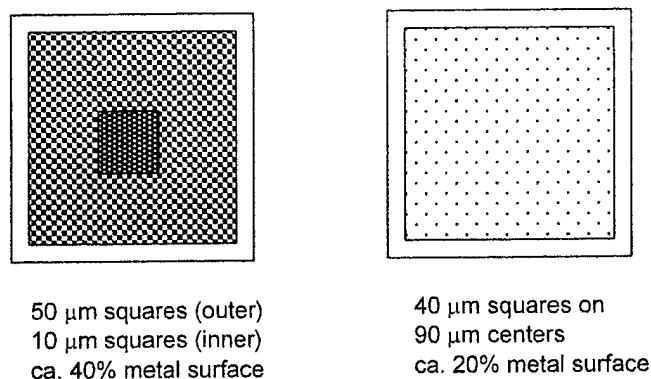


Figure 6 Platinum and palladium patterns on n-type silicon substrates.

Vapor deposition of patterned and unpatterned palladium thin films ($\sim 2\text{ nm}$). In addition to platinum, palladium coatings were also examined. These had slightly better performance than the platinum. That is, unpatterned palladium thin films were stable to oxidation for about 30-60 min during potential cycling in 50 mM histidine but, unfortunately, exhibited relatively high background currents (Figure 7a). Patterned films (pixelation) showed no stabilizing effect at all (Figure 7b). Since the patterned palladium thin film covered only a fraction of the silicon surface (Figure 6), it was expected that the photocurrent would decay initially then stabilize as the oxidation of the silicon became saturated. However, a stable plateau region at reduced photocurrent levels was not observed. This phenomenon was not investigated further but it is likely that the lack of a stable photocurrent is related to strong Fermi level pinning at the edges of the Pd patterns. Fermi level pinning prevents the build-up of a junction potential and therefore a photocurrent. It is known to occur frequently at surface defect sites.

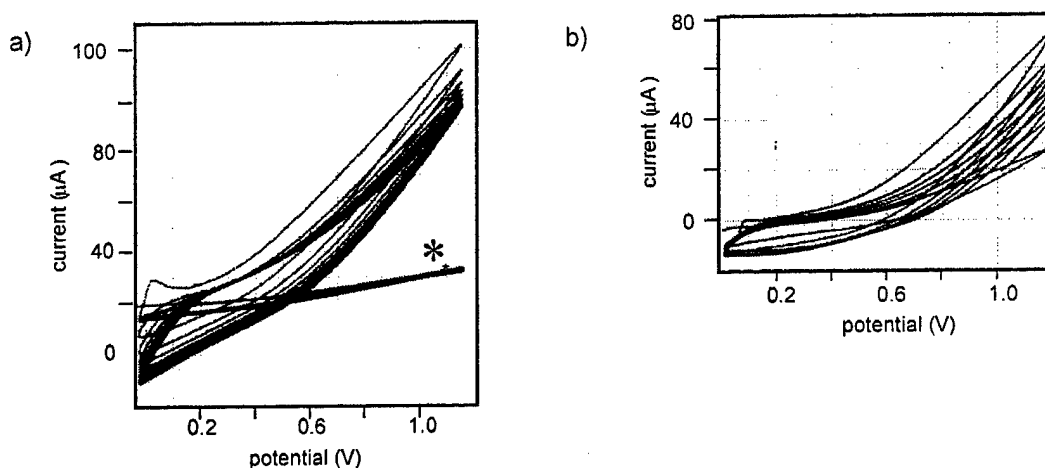


Figure 7. Cyclic voltammograms of a) n-type silicon with 2 nm Pd (photoresponse & relatively stable) and b) n-type silicon with 2 nm patterned Pd (photoresponse but poor stability), * = dark current

Solution deposition of Mn_2O_3 ($MnO(OH)$) films. This is one of the few systems with long term stability reported in the literature. After introducing several changes to a procedure published by Bockris, et al., we were able to stabilize n-type silicon substrates ($1-4 \Omega \text{ cm}$ resistivity) against oxidation. In brief, the procedure entails depositing a seed layer of palladium onto a silicon surface then precipitating $MnO(OH)$ on top of the palladium. The $MnO(OH)$ is converted to Mn_2O_3 by heating *in vacuo*. The long-term stability of substrates covered with an approximately 300 nm thick layer of Mn_2O_3 is excellent as seen in Figures 8a and 8b. Potential cycling in 50 mM histidine can be performed for many hours without observing a significant decrease in photocurrent.

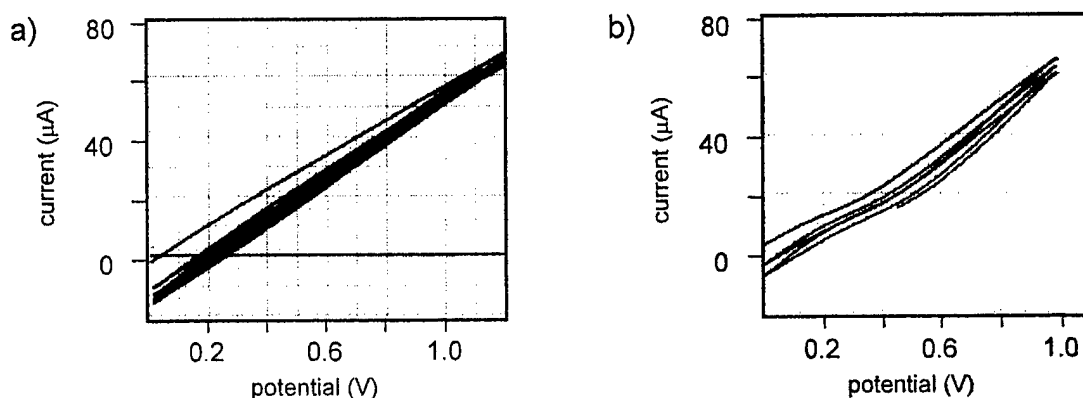


Figure 8. Cyclic voltammograms of a) n-type Si covered with thin layers of Pd and manganese oxide (good photoresponse and stable) and b) same sample after a stability test at 1V for about 70 minutes (good photoresponse and stable).

Part of this stability may be inferred from an atomic force microscope (AFM) image of the Mn_2O_3 surface (Figures 9 and 10). As can be expected from a precipitation process, the film has a granular structure with lateral grain sizes ranging from 1 to 3 microns and a mean roughness of about 100 nm (z-axis). Some crystallites at the surface of the film have larger diameters that give rise to an apparent thickness of 1.6 μm . Therefore the silicon surface is apparently well protected by this relatively thick layer of Mn_2O_3 . Supporting this view is the observation that there are only few observable defects or pinholes (optical microscope).

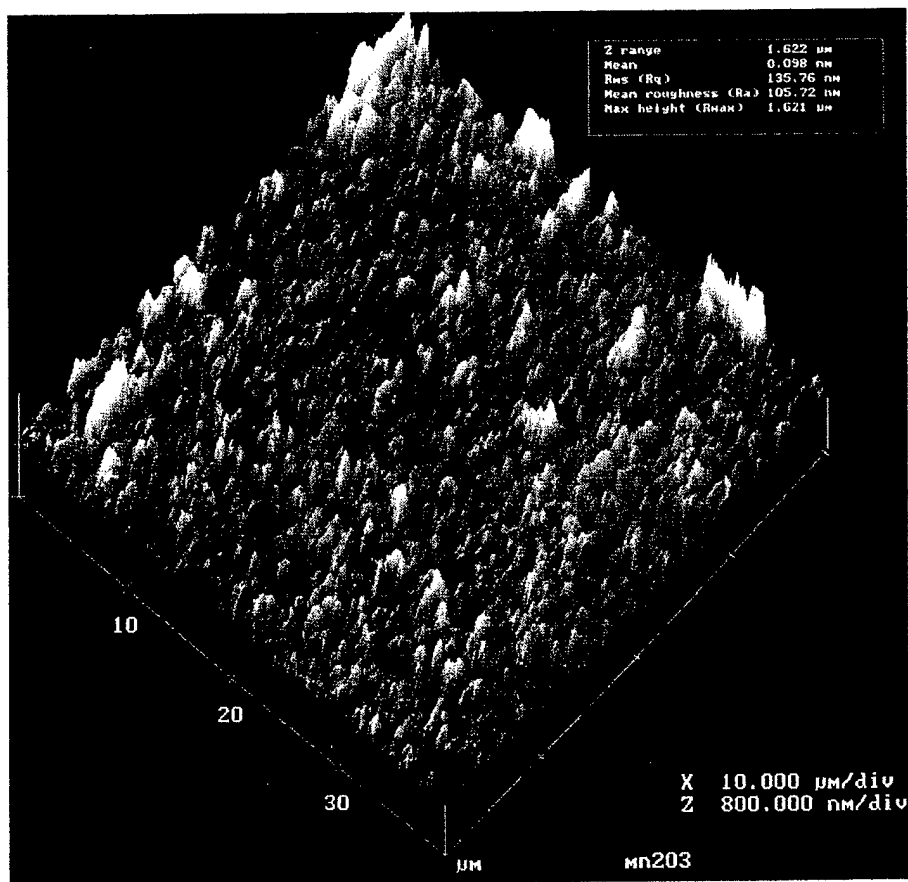


Figure 9. AFM surface plot of a Mn_2O_3 thin film ($40\text{ }\mu\text{m} \times 40\text{ }\mu\text{m}$).

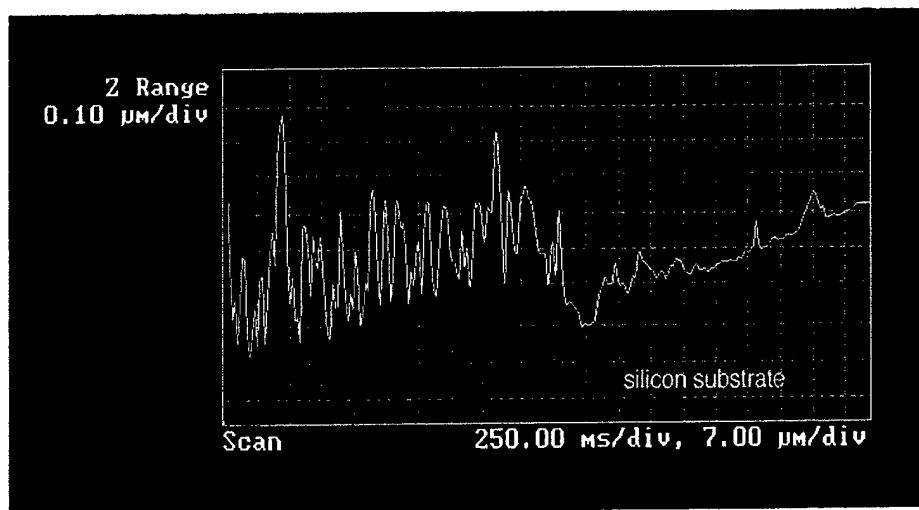


Figure 10. AFM profile of the edge region of a Mn_2O_3 thin film.

In summary, of the surfaces examined, the Mn_2O_3 coating exhibited the best photooxidation stability and photoresponse. Therefore, this surface coating on n-type silicon was chosen for further development of the photowrite process.

Several test experiments were performed in order to demonstrate electrophoretic transport using the photo-write process. A first set of experiments demonstrated the accumulation of fluorescence labeled DNA oligonucleotides on a Mn_2O_3 surface. In brief, these consisted of applying a potential (either constant or varying) across the electrolyte from the electrode to the silicon chip. A portion of the photoreactive surface was then illuminated using the fiber optic. If working, a current would be observed between the point of illumination and the electrode, generating the electrophoretic force necessary to mobilize negatively charged materials to the point of illumination. Figure 11a shows fluorescence images taken with a CCD camera before and after the application of a constant electrochemical potential. Figure 11b illustrates the change of fluorescence during the same experiment. (The oligonucleotides diffuse away in absence of an applied potential since the Mn_2O_3 layer does not offer any attachment sites.) While the DNA experiments showed accumulation, they did not provide any information on the spatial distribution of the photocurrent since the fluorescence was only monitored within the illuminated spot.

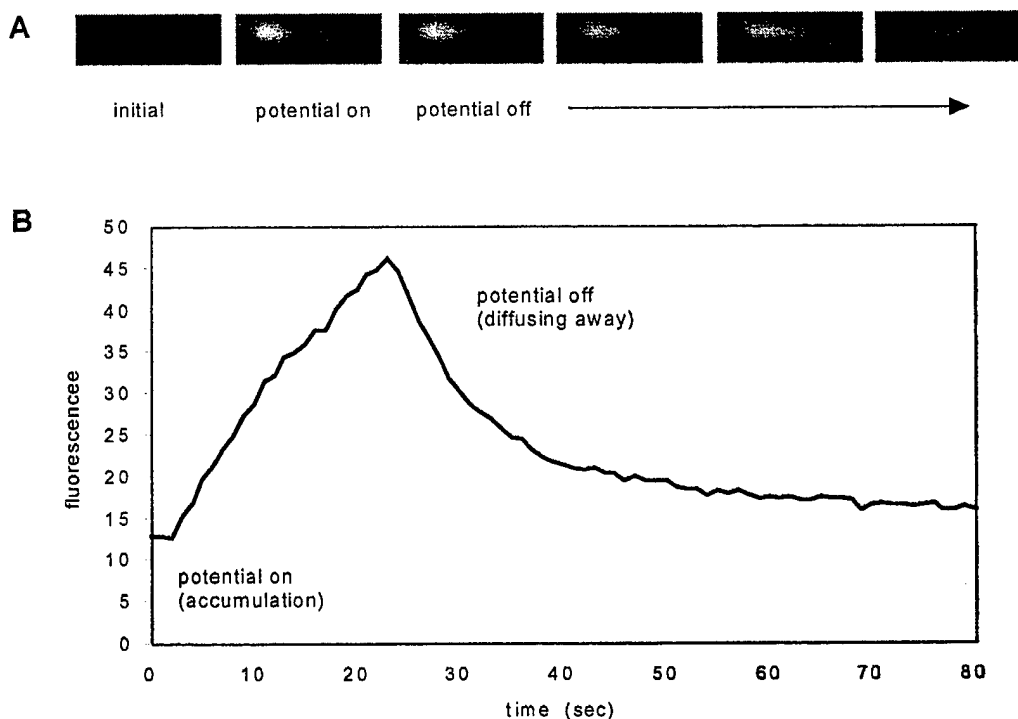


Figure 11. a) Fluorescent DNA oligonucleotide accumulation by the photo-electrochemical write process. b) Fluorescence level detected at the illuminated spot during the accumulation experiment.

In a second series of experiments, continuous lines of conducting polypyrrole were created on a Mn_2O_3 stabilized n-type silicon chip by moving the fiber optic on the XYZ stage while applying a potential. The lines were produced by inducing photo-electrochemical oxidation of pyrrole (0.2 M pyrrole and 0.1 M LiClO_4 in water) at specific locations illuminated by the scanned optical fiber. (Figure 12) The appearance of the lines demonstrated that the photocurrents are fairly localized and that the substrate has continuous photoactivity. Polypyrrole lines are expected to be rather wide because of the conducting nature of this polymer.

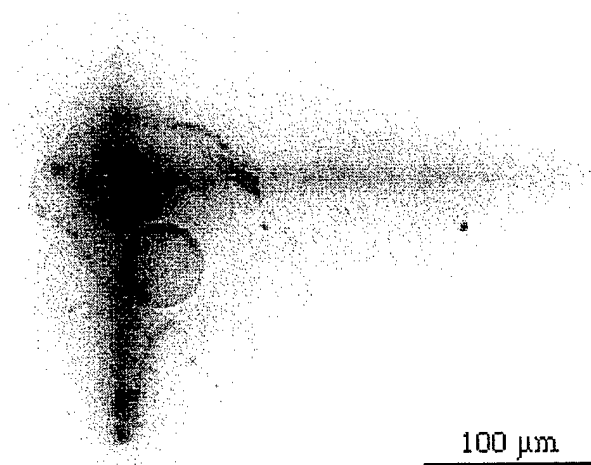


Figure 12. Polypyrrole lines produced by the photo-electrochemical write process

A final series of transport and accumulation experiments were performed with fluorescent and non-fluorescent polystyrene beads (1-10 μm dia) functionalized with carboxylic acid groups. Figure 13a shows a Mn_2O_3 surface immersed in 50 mM histidine containing 1 μm diameter non-fluorescent polystyrene beads. The surface is illuminated by the single-mode optical fiber producing an illuminated spots size of about 30 μm . The relatively large spot size is due to scattering off the polystyrene beads. Figure 13b shows the same spot after cycling the applied potential between 0 and 1.2 V for 1 min. There is clear accumulation of beads in a very limited area where the surface was illuminated by the laser light. Figure 14 shows the result of similar experiments performed under slightly different conditions. It can be seen that the number of beads accumulated during illumination is dependent on the photocurrent which is a function of both the applied potential and the illumination intensity.

It was noted that the application of a constant (in contrast to scanned) potential did not result in efficient bead accumulation. This might be attributable to the tendency of the beads to stick to the surface around the illuminated spot when attracted by a constant electric field (photocurrent and dark current). In

experiments with fluorescence labeled DNA molecules, similar results were obtained with either scanned or constant potentials (see above). On some of the substrates, bead movement could be induced even in absence of an applied potential. This is possible since the photoactive surface can act as an anode in one location and as a cathode in another location allowing for local current flow without the support of external circuitry. This effect is not observed in solutions with higher electrical conductivity (mS/cm) ruling out a thermal or convection mechanism.

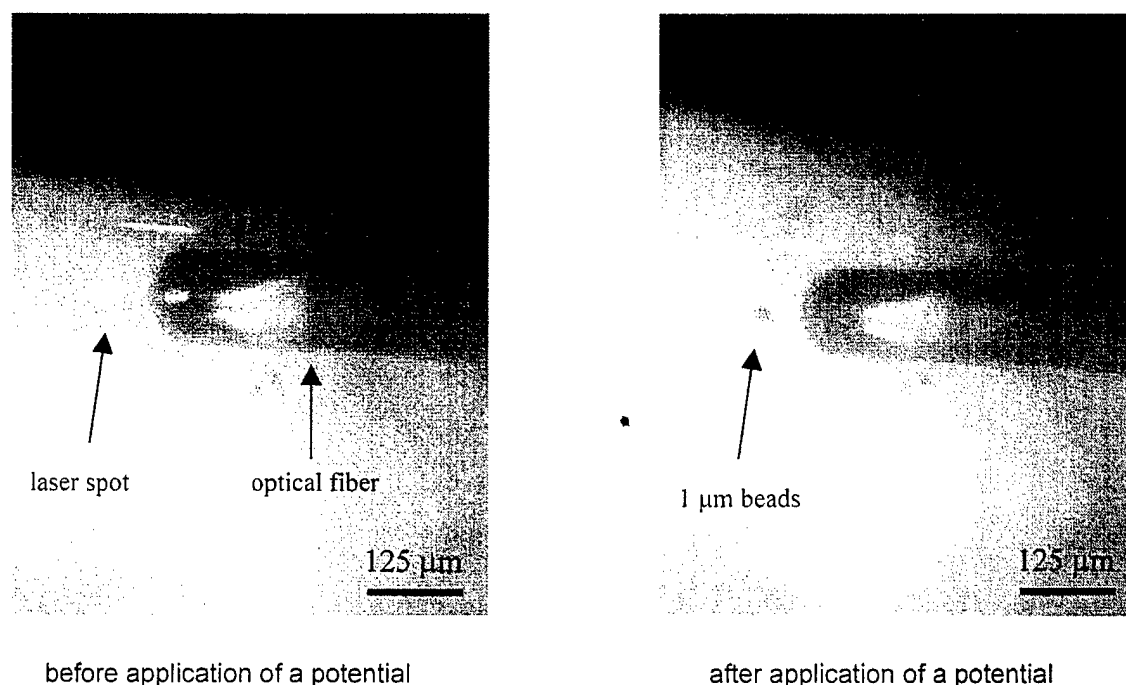


Figure 13. Bead movement induced by photo-electrochemical currents.

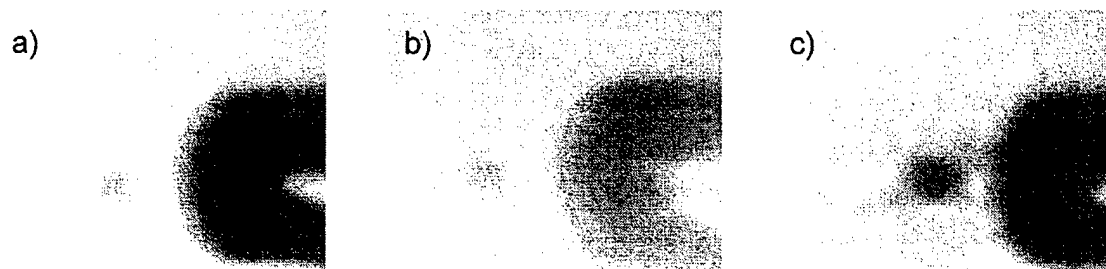


Figure 14. Accumulation of 1 μm diameter polystyrene beads under different conditions: a) 0-0.6V scanned potential, 80 μW illumination, 1min; b) 0-1.2 V scanned potential, 80 μW illumination, 1 min ; c) 0-1.2 V scanned potential, 200 μW illumination, 1 min.

c) Attachment of DNA Oligonucleotides: 4.1.1.2 Attach DNA sequences to selected photoactive substrate materials.

Previous research performed at Nanogen demonstrates that electronic hybridization of oligonucleotides to DNA capture strands directly linked to an electrode surface is not efficient. In order to protect the oligonucleotides from the harsh environment during water electrolysis and to create favorable conditions for DNA hybridization, it is necessary to coat the electrode surface with a permeation layer. Several types of proprietary permeation layers previously developed at Nanogen were tested in combination with Mn_2O_3 stabilized n-type silicon substrates. Unfortunately it was found that the deposition of the permeation layers destroyed the stabilizing effects of Mn_2O_3 or that the permeation layers exhibited very poor adhesion. Three strategies were pursued to overcome the observed problems: First, it was tried to alter the permeation layer chemistry and the permeation layer deposition process to avoid chemical degradation of the Mn_2O_3 surface. Second, the published procedure for Mn_2O_3 deposition was altered in order to increase stability. Third, Mn_2O_3 surfaces were treated with various chemical agents to improve adherence of the permeation layer. The use of altered permeation layers dramatically improved the stability of the photoactive substrates. However, the yields for chemical attachment of DNA capture strands were less than satisfying. Better overall success was achieved by altering the Mn_2O_3 deposition process. In brief, the deposition was optimized for film adherence, film homogeneity, reproducibility and ease of processing. Mn_2O_3 layers deposited with this modified procedure had sufficient-to-excellent stability even after coating with a standard permeation layer and after chemical attachment of DNA capture strands. (Figure 15) A moderate increase in dark current was still observed but this was not a major problem.

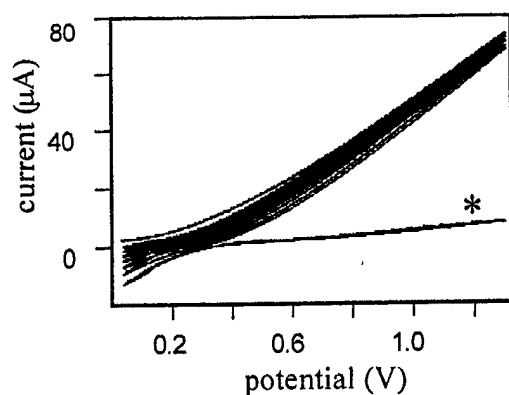


Figure 15. Cyclic voltammogram of a Mn_2O_3 stabilized silicon substrate covered with a permeation layer (measured in 50 mM histidine, scanning rate 200 mV/sec), * = dark current.

Surface treatment of Mn_2O_3 layers also had a positive effect on the adhesion of certain kinds of permeation layers and did not seem to affect the stability of the protecting layer. After successfully resolving these compatibility issues, attachment of DNA capture strands through a standard biotin/streptavidin interaction did not pose any additional problems. A cross section of the final structure of the photo-write platform is shown in Figure 16.

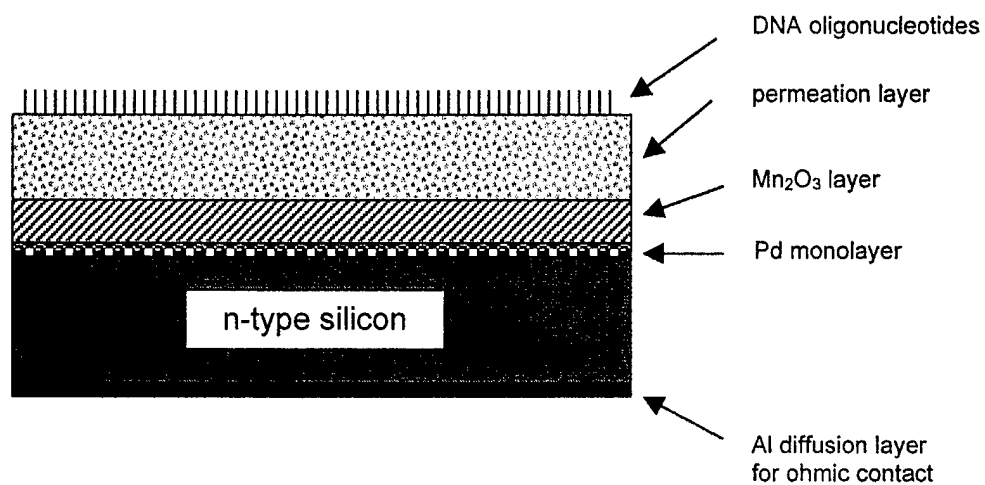


Figure 16. Schematic view of the structure of the photowrite platform.

d) Demonstrate and Evaluate the Photowrite Process:

4.1.2 Demonstrate the photo-electronic write process on DNA sequences attached to photoactive substrate materials. 4.1.3 Demonstrate spectral read-out process of DNA sequences attached to photoactive substrate materials. 4.1.4 Optimize the size of the write locations (4.1.2) and demonstrate the photo-electric write/read process in pixel format.

There are three basic strategies for the introduction of fluorescent dyes utilizing the photowrite process as outlined in Figure 17:

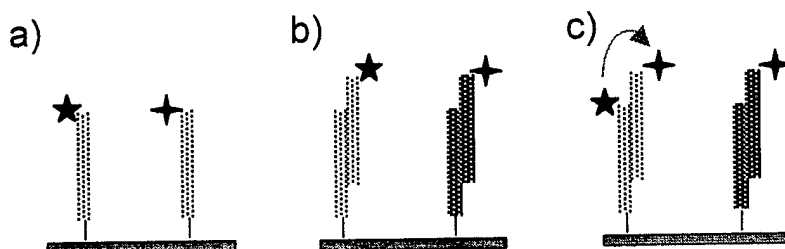


Figure 17. Basic configurations for the introduction of fluorescent dyes utilizing the photowrite process (star symbols indicate tethered fluorescent dye molecules).

As shown in Figure 17, these three approaches are: a) DNA oligonucleotides derivatized with different kinds of fluorescent dyes can be introduced sequentially and bound to the permeation layer surface using a non-covalent biotin/streptavidin interaction. This strategy has an advantage in that it is relatively fast (no passive hybridization step) and that it requires only very low concentrations of oligonucleotides. On the negative side, problems with photobleaching are to be expected (see below). b) As a first step, different sequences of unlabeled DNA oligonucleotides are sequentially bound to the permeation layer (photowrite step). In a second step, a mixture of labeled, complementary DNA oligonucleotides is added and allowed to hybridize with the capture strands on the surface. This strategy avoids any photobleaching effects but involves a relatively slow passive hybridization step. c) This strategy is a combination of the above methods that allows for additional complexity by introducing fluorescence resonant energy transfer (FRET). Fluorescence resonant energy transfer involves excitation of one fluorescent dye followed by transfer of the excitation energy onto a second dye that emits at a different wavelength. Overall, this may allow for multiple fluorescent emission using only a single excitation source.

A basic demonstration of the photowrite process was first attempted using fluorescence labeled/biotinylated DNA oligonucleotides (strategy depicted in Figure 17a). As mentioned above, photobleaching was expected to be a problem when using dyes that absorb at the wavelength of the laser emission. Preliminary experiments on microelectrode arrays revealed that even minimal overlap of the absorption spectra with the laser emission line can lead to observable photobleaching effects. It was found that BODIPY TR-X (588/616) is efficiently bleached not only by a 594 nm laser but also by a 630 nm laser. No bleaching was observed for a blue fluorescent dye (493/503 nm) in combination with a 630 nm laser. This is shown in Figure 19a by the corresponding increased intensity of targeted blue labeled material with greater illumination. In contrast, BODIPY TR-X (588/616) bleached or lost intensity with increased intensity. Figure 19b indicates that the loss of signal was not due to direct damage of the oligonucleotides since non-labeled, irradiated oligonucleotides supported subsequent hybridization with fluorescently labeled oligonucleotides.

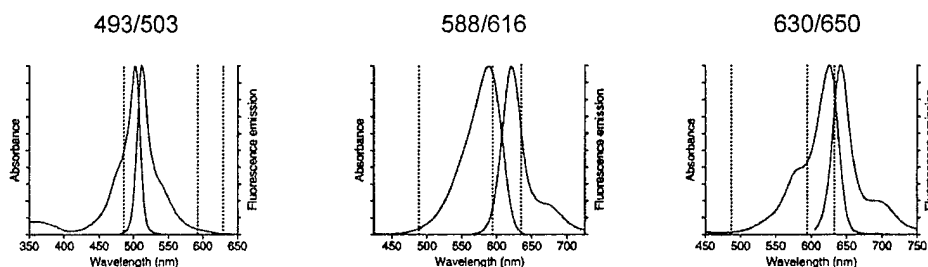


Figure 18. Absorption and emission spectra of fluorescent dyes used. Vertical lines indicate photowrite laser wavelengths.

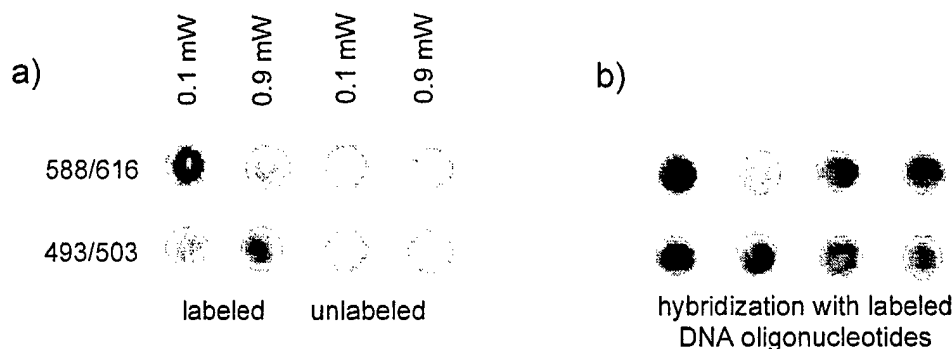


Figure 19. Effect of 630 nm laser irradiation during electronic binding (biotin/ streptavidin) of labeled and unlabeled DNA oligonucleotides.

Based on these findings, it was determined that, in combination with the far red 630 nm laser, it is possible to directly photowrite oligonucleotides labeled with the blue 493/503 dye and avoid serious photo-bleaching. Examples of fluorescent spots and lines produced by this form of the photowrite process using DNA oligonucleotides labeled with this dye (0.2 μ M in 50 mM histidine) are shown in Figure 20.

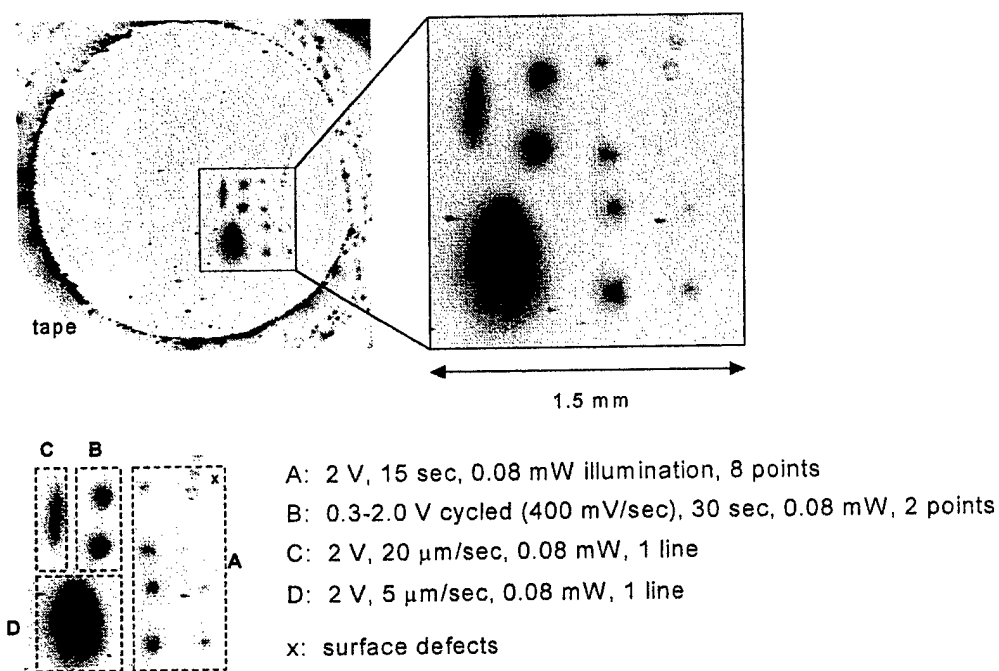


Figure 20. Fluorescent patterns produce by the photowrite process under various conditions.

The left side of Figure 20 shows a fluorescence scanning image of the photowrite substrate after a series of photowrite experiments. The circular region defined by a piece of plastic tape is the part of the surface that was exposed to the solution during the experiment. The right side shows a magnified view of the fluorescent photowrite patterns produced under various conditions:

Fluorescent patterns can be generated with constant as well as with cycled potentials. This is in accordance with the accumulation experiments described above (section IIIc). Fluorescent lines can be produced by simply scanning the optical fiber across the permeation layer surface. Figure 21 shows fluorescence intensity contour plots of some of the patterns in Figure 20. As can be expected, fluorescent spot sizes and intensities vary with applied potential and illumination intensity (see below) but

also with illumination time and between different spot locations. Exact correlation between the different parameters and the resulting spots could not be obtained because of large variations in behavior between different samples.

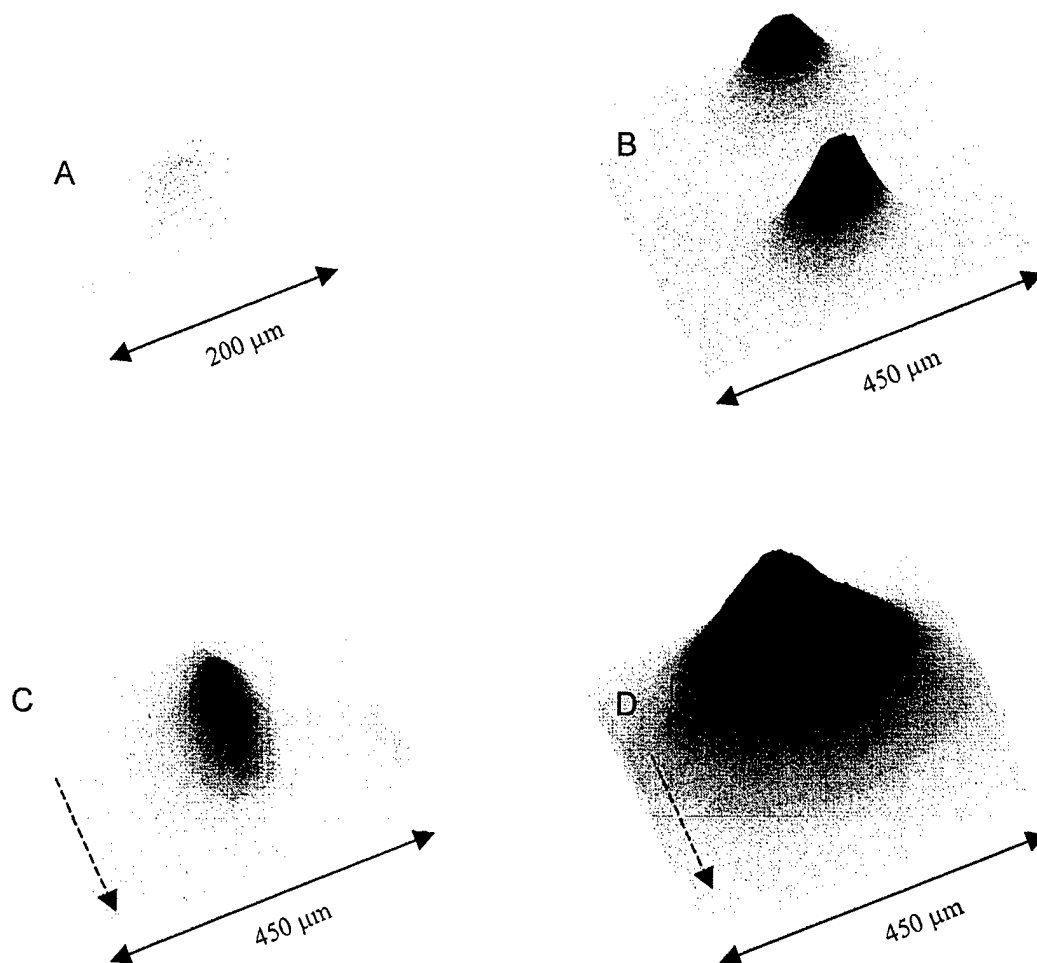


Figure 21. Fluorescence intensity contour plots of photowrite patterns in Figure 20. The dashed arrows in images C and D indicate the scanning direction of the optical fiber.

The results described above demonstrate the successful generation of single color fluorescent patterns by the photowrite process following the strategy outlined in Figure 17a. A demonstration of a two color fluorescent pattern involving fluorescent resonant energy transfer (see also Figure 17c) is given in the following section:

As a first step, a solution of biotinylated, blue fluorescent (493/503) labeled oligonucleotides (400 nM) was applied to a permeation layer covered photoactive substrate. Several fluorescent spots separated by

400 μm were then sequentially generated by applying 1.5 V for 1 min using an illumination intensity of 0.09 mW (633 nm). In a second step, biotinylated but unlabeled DNA oligonucleotides were deposited in adjacent locations applying the same conditions. A solution containing red fluorescent dye (630/650) labeled oligonucleotides complementary to the already targeted and anchored strands (2 μM in 0.1 M phosphate buffer pH 7.4) was then added and hybridized for 1 hour (Fig. 24). The fluorescent dyes were chosen to minimize non-intended absorption/excitation by the laser wavelengths used for excitation (see Figure 20). The sample was analyzed using a 488 nm and a 630 nm laser source combined with 505 nm and 670 nm band pass emission filters (Figure 25).

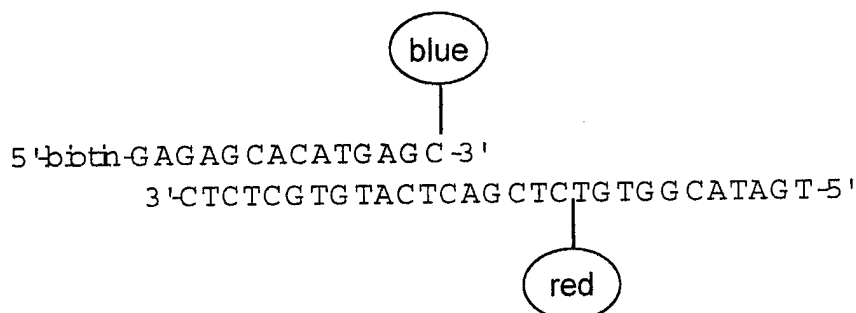


Figure 24. Combination of dyes and oligonucleotides demonstrating fluorescent resonant energy transfer.

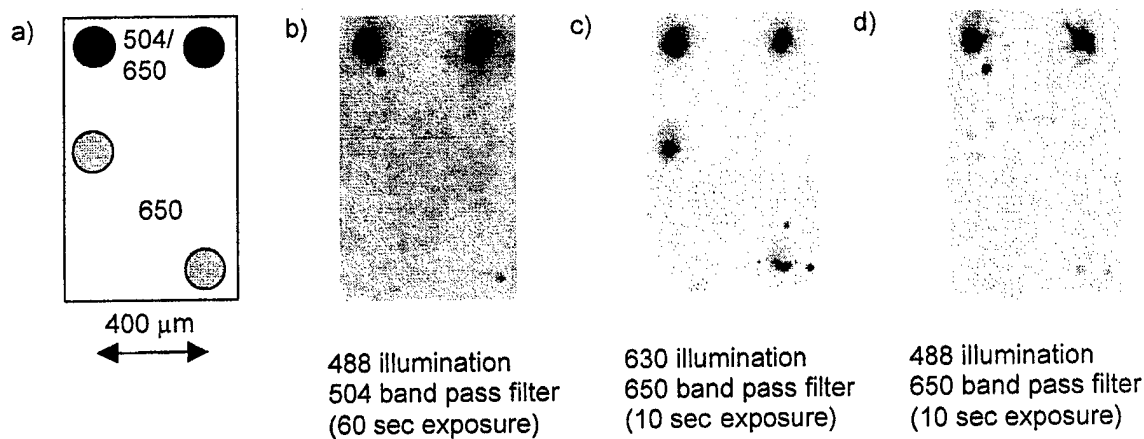


Figure 25. Example of a two color photowrite pattern. a) DNA oligonucleotide positions, b) detection of the blue dye, c) detection of coupled and uncoupled red dye, d) detection of the red dye coupled by fluorescence resonant energy transfer to the blue dye.

As shown in Figure 25, fluorescence emitted by the blue dye molecule was detected by illumination with a 488 nm laser using a 505 nm emission band pass filter (Figure 25b). The fluorescence intensity was

relatively low (requiring a long exposure time) since part of the excitation energy was quenched by the red dye present on the hybridized complementary strand. Hybridized DNA oligonucleotides (derivatized with red dye molecules) were detected by illumination with a 630 nm laser using a 670 nm emission band pass filter (Figure 25c). Finally, fluorescence resonant energy transfer was demonstrated by illuminating again with a 488 nm laser but using the 670 nm emission band pass filter for detection of the red dye. In this case, only those red dye molecules that are in close proximity to blue dye molecules, i.e. by hybridization, emit fluorescent light (Figure 25d).

It is therefore possible to not only photowrite multiple colors to different locations but also to introduce additional spectral complexity to the photowrite process by using fluorescence resonant energy transfer in combination with a series of photowrite and passive hybridization steps.

e) **Demonstration/Reports/Evaluation:** 4.1.5 Deliver a photo-electric write/read breadboard model demonstration system. 4.1.6 Continually determine the status of the effort and report progress towards accomplishment of contract requirements. 4.1.7 Conduct oral presentations at such times and places designated in the contract schedule. Provide status of technical progress made to date in performance of the contract during presentations. Contractor presentations will be attended by approximately two (2) Government personnel. 4.1.8 Conduct an experimental demonstration exhibiting paragraphs 4.1.2 and 4.1.3; and an experimental demonstration exhibiting paragraph 4.1.4 at the end of the contract period. Document each experiment on video tape.

A site visit was conducted by two Air Force Research Laboratory representatives, Dr. Ed Daniszewski and Mr. Albert Jamberdino, during September 1998. Additional reports, both before and after this visit, have been supplied to Dr. Daniszewski on a regular basis and a final summary of the work was presented at the 44th annual SPIE meeting in Denver, CO on July 22, 1999. (Mr. Jamberdino was present.) The model write system, schematically outlined in Figure 1, is shown in the accompanying videotape.

f) **Documentation:** 4.1.9 Document all technical work accomplished and information gained during performance of this acquisition. Include all pertinent observations, nature of problems, positive and negative results, and design criteria established where applicable. Document procedures followed, processes developed, "Lessons Learned," etc. Document the details of all technical work to permit full understanding of the techniques and procedures used in evolving technology or process developed. Cross-reference each design, engineering, or process specification delivered to permit a full understanding of the total acquisition.

Progress and data on this project is maintained in individual laboratory notebooks as well as in electronic files and on videotapes at Nanogen. A videotape with experimental demonstrations is being supplied with this report.

V. Conclusions

The aim of this contract was to develop a platform for spatially localized photoelectrophoretic movement and placement of fluorescently labeled DNA oligonucleotides and micromaterials derivatized with DNA oligonucleotides. This involved the development of a photoactive substrate that provides binding sites for DNA oligonucleotides and that is chemically and electronically stable in aqueous environment under conditions of water electrolysis. It also involved the construction of an electronically controlled high-resolution optical write/read system.

We have successfully stabilized photoactive crystalline silicon surfaces by depositing thin films of Mn_2O_3 . The stabilized surfaces were covered with hydrogel permeation layers offering attachment sites for DNA oligonucleotides (through a biotin/streptavidin interaction) and that protect the oligonucleotides from chemically reactive electrolysis products. This novel photoactive substrate was used to enable photoelectrophoretic transport and anchoring of fluorescently labeled and unlabeled biotinylated DNA oligonucleotides. Photocurrents were generated by illumination with a single-mode optical fiber mounted on an electronically controlled micropositioning system. By applying this process, one and two color fluorescent spots and lines (FWHM about $50\text{ }\mu\text{m}$) were generated and read out with either a high-resolution optical scanner or a CCD camera. Two color emission from illumination with a single excitation source was accomplished by enabling fluorescence resonant energy transfer (FRET) between different fluorescent dye molecules attached to complementary DNA strands. Photo-electrophoretic movement and positioning of micrometer sized polystyrene beads was demonstrated as well.

This contract has provided a proof-of-principle demonstration of photo-electrophoretic transport and binding of DNA oligonucleotides. The next stage to developing this technology further might focus on two areas. The first of these is that the stabilization of silicon substrates with Mn_2O_3 thin films could be improved in order to enhance reproducibility and homogeneity of the photocurrent response. This is anticipated to involve modification of silicon substrate pretreatment and Mn_2O_3 deposition as well as modification of permeation layer chemistry. The second area possibly to be examined is to sharpen the spatial resolution of the photowrite process. The current resolution is about $50\text{ }\mu\text{m}$. Further decrease of the illumination spot size (lenses, thinner permeation layer) combined with a reduction of photocurrent spread (lower resistivity substrates, patterning) should allow for an improved resolution of at least $10\text{ }\mu\text{m}$. In conclusion, even at its present state of development, we have shown the photowrite process to be a novel, freely controllable means of positioning fluorescent materials and should provide one method for assembling even more complex photonic structures upon a two dimensional surface.

Appendix A: Oligonucleotide Sequences

- 1) 5' biotin-gag agc aca tga gt(NH₂)c – 3'
- 2) 5' – tga tac ggt gt(NH₂)t ctc gac tca tgt gct ctc – 3'
- 3) 5' biotin - ttt ttt ttt ttt(NH₂) – 3'
- 4) 5' biotin - gat gag cag ttc tac gtg g – 3'
- 5) 5' - (NH₂)cca cgt aga act gct cat c – 3'
- 6) 5' – t(CO)t(CO)t(CO) gag agc aca tga ctc – 3'
- 7) 5' – t(CO)t(CO)t(CO) gat gag cag ttc tac gtg g – 3'
- 8) 5' - gag aac acc gt(NH₂)a tca gat cag caa gca gac – 3'
- 9) 5' – gtc tgc ttg ctg at(NH₂)c – 3'

biotin = site of biotinylation.

NH₂ = C6 side chain with a primary amine (for dye attachment).

CO = carboxylic acid group on side chain.

Appendix B: Description of Video Tape Contents

(0:00 min) Instrumental Setup

Photowrite Setup: This image shows the electrochemical assembly (see Figure 2) and the microscope on the left hand and the micromanipulator controller on the right hand.

Free Space Optical Fiber Launch: The laser is on the right side, a neutral density filter wheel in the center, and the actual single mode optical fiber launch can be seen on the left side.

Electrochemical Assembly with Single Mode Optical Fiber: A close-up of the photowrite set-up with microscope lenses in the upper half, the electrochemical assembly is in the center, and the single mode fiber with fiber chuck attached to the micromanipulator arm on the left side (see Figure 1).

(0:32 min) Fluorescently Labeled DNA Accumulation

This sequence shows accumulation of fluorescently labeled DNA oligonucleotides on a Mn_2O_3 coated n-type silicon substrate (no permeation layer). The fluorescent thin red line at the beginning of the sequence marks the path of the laser light originating from the single mode fiber. The fluorescence intensifies at the Mn_2O_3 surface (round spot) during application of a potential of 1 V due to accumulation of labeled oligonucleotides (see Figure 11). The accumulated oligonucleotides diffuse again away after the potential is turned off. The end of the sequence shows movement of the optical fiber across the surface.

(1:20 min) Bead Movement Experiments

The three sequences compare transport behavior of fluorescently labeled polystyrene beads (3 μm diameter) at open circuit, at applied constant potential and at applied scanned potential (see section IVc and Figure 14) The experiments were performed on a Mn_2O_3 covered n-type silicon substrate (no permeation layer).

Bead Movement Without Applied Potential: The first few seconds display a close-up of the optical fiber (125 μm diameter) above the Mn_2O_3 surface (microscope light is on). Upon irradiation with laser light, some fluorescent beads start slowly moving towards the illuminated spot. Scanning of the fiber across the surface demonstrates how beads can be transported.

Bead Movement with Applied Constant Potential: Application of a constant potential of 1V leads to only very little bead movement (see text).

Bead Movement with Applied Scanned Potential: This time compressed sequence shows the same spot as above before, during and after application of a scanned potential (0-1.2V, 400 mV/sec). The application of a scanned potential produces a more efficient accumulation than the static potential. The end of the sequence shows the accumulated beads diffusing away as the potential is set to 0 V.

***MISSION
OF
AFRL/INFORMATION DIRECTORATE (IF)***

The advancement and application of information systems science and technology for aerospace command and control and its transition to air, space, and ground systems to meet customer needs in the areas of Global Awareness, Dynamic Planning and Execution, and Global Information Exchange is the focus of this AFRL organization. The directorate's areas of investigation include a broad spectrum of information and fusion, communication, collaborative environment and modeling and simulation, defensive information warfare, and intelligent information systems technologies.